Nuclear-Quadrupole-Resonance Study of Lattice Dynamics in K_2PtCl_6†

K. R. JEFFREY* AND R. L. ARMSTRONG
Department of Physics, University of Toronto, Toronto, Canada

(Received 29 April 1968)

A pulsed magnetic-resonance spectrometer is used to measure pure NQR frequencies and relaxation times of the ^{35}Cl and ^{37}Cl nuclei in powdered samples of K_2PtCl_6 over the temperature range $6<T<490°K$. The ratio of frequencies is independent of temperature and equal to 1.2688 ± 0.001, in agreement with the ratio of quadrupole coupling constants as found for free Cl atoms. It is shown that a single low-frequency vibrational mode of frequency ~38 cm^{-1} dominates the motional averaging of the electric field gradient at a Cl site. This mode is identified as the rotary lattice mode which corresponds to the threefold degenerate torsional oscillations of the $[PtCl_6]^{=}$ ion. A realistic model of the field gradient is proposed, and the data are discussed in terms of this model. The T_1 data span seven orders of magnitude from 100 μsec at 490°K to 20 min at 6°K. For $T<320°K$, $T_1(^{37}Cl)/T_1(^{35}Cl)\simeq1.6$; for $T>320°K$, $T_1(^{35}Cl)=T_1(^{37}Cl)$. For $6<T<90°K$, the temperature dependence of T_1 is consistent with the Van Kranendonk theory, assuming that the relaxation is dominated by a single optical mode of frequency ~33 cm^{-1}, that is, by the rotary lattice mode. For $90<T<320°K$, the T_1 data increase more slowly with temperature than can be accounted for by the Van Kranendonk theory. This is thought to be because the amplitude of the torsional oscillations has become so large as to invalidate the assumptions of a harmonic theory. For $320<T<490°K$ the T_1 data suggest that the energy of the torsional oscillations has become sufficient for the onset of a hindered rotational motion. This would lead to a nonresonant relaxation process and a T_1 determined solely by the residence time of a $[PTCl_6]^{=}$ ion in one of its equilibrium orientations. An order-of-magnitude calculation gives support to such an interpretation. The T_2 data are dominated by a magnetic dipolar spin-spin interaction. This is verified experimentally by observing the magnetic field dependence of the spin-echo beats.

1. INTRODUCTION

THE Hamiltonian describing the interaction of a nuclear quadrupole moment **Q** with the local electric field gradient $\nabla\mathbf{E}$ as found in crystalline solids can be written

$$\mathcal{H}_Q=\sum_{\mu=-2}^{2}Q_\mu\nabla E_\mu,$$

where the Q_μ are the components of **Q** and ∇E_μ are the components of $\nabla\mathbf{E}$. The field gradient can be expanded in terms of the displacements of the nuclei from their equilibrium positions[1] r_i° as

$$\nabla E_\mu=A_{0\mu}+\sum_i A_{1\mu}:r_i^\circ+\sum_{ij}A_{2\mu}:r_i^\circ r_j^\circ+\cdots.$$

The first term, which is a constant, determines the "zero motion" pure nuclear-quadrupole-resonance (NQR) energy levels. The higher-order terms are responsible for the temperature variation of the NQR frequency and for quadrupolar spin-lattice relaxation processes. The time average component of the field gradient, taken over times short compared to the reciprocal of the resonance frequency, determines the NQR frequency.[2–4] This average field gradient is temperature-dependent because the amplitudes of the lattice vibrations and the volume of the sample change with temperature. Quadrupolar relaxation is brought about by the transitions induced by the time-dependent parts of the Hamiltonian. The linear term gives rise to a direct spin phonon interaction. This provides a very inefficient relaxation mechanism because of the small number of rf phonons in a crystal. The quadratic term gives rise to two phonon processes of which the Raman spin phonon process is by far the most important. In the Raman process, one phonon is created, another annihilated, and a nuclear spin flip occurs. This provides a very efficient relaxation mechanism since the entire phonon spectrum can participate. Recently, it has been shown that another Raman process is important in which a three-phonon interaction, resulting from anharmonicities in the lattice vibrations, combines with a direct process.[5] Both Raman processes are predicted to have the same temperature dependence.

Although NQR frequencies have been measured in a large variety of substances, relatively few of these measurements are on substances in which the bonding is ionic or covalent. Some of the more recent work of the latter type includes measurements on Cu_2O,[6] LaF_3,[7] and $HgCl_2$.[8] The experimental results are reasonably well explained by the theory.

Quadrupolar relaxation has been studied extensively

† Research supported in part by a grant from the National Research Council of Canada.

* Holder of an E. F. Burton Fellowship in the School of Graduate Studies, University of Toronto.

[1] J. Van Kranendonk, Physica **20**, 781 (1954).

[2] H. Bayer, Z. Physik **130**, 227 (1951).

[3] T. Kushida, J. Sci. Hiroshima Univ. **A19**, 327 (1955).

[4] T. Kushida, G. B. Benedek, and N. Bloembergen, Phys. Rev. **104**, 1364 (1956).

[5] J. Van Kranendonk and M. Walker, Phys. Rev. Letters **18**, 701 (1967).

[6] H. W. De Wijn and J. L. De Wildt, Phys. Rev. **150**, 200 (1966).

[7] K. Lee, A. Sher, L. O. Anderson, and W. G. Proctor, Phys. Rev. **150**, 168 (1966).

[8] Dinesh and P. T. Narashinham, J. Chem. Phys. **45**, 2170 (1966).

in cubic compounds where there is no static quadrupolar interaction such as the alkali halides[9] and compounds of the zinc-blende structure.[10,11] The temperature dependence of the spin-lattice relaxation time is well explained by the theory if both acoustical and optical phonons are considered. Usually a Debye spectrum is used to represent the phonon spectrum of the acoustical modes and Einstein phonon distributions to represent the optical modes.

Very few investigations of quadrupolar relaxation in ionic or covalent substances where there is a pure NQR spectrum have been reported. Recently, measurements on Cu_2O[12] and substances with the RXO_3 structure[13] have been carried out and analyzed, using the available theory.

Most ionic or covalent compounds which have a pure NQR spectrum have a complex structure. The analysis of the results might therefore be expected to be very difficult unless, of course, a small number of lattice vibrations dominate the behavior of the NQR frequencies and relaxation times. In such cases an analysis of NQR experiments can yield detailed information about these modes.

In this paper the results of NQR experiments in the temperature range 6 to 490°K on the ^{35}Cl and ^{37}Cl nuclei in K_2PtCl_6 are presented and analyzed. The only previous work on this substance consists of measurements of the ^{35}Cl resonance frequency at a few temperatures between 77 and 300°K.[14,15] In Sec. 2 the experimental apparatus and techniques are discussed. The nature of the field gradient at a Cl site is considered in Sec. 3. Presentations and discussions of the frequency data and the spin-lattice relaxation-time data are given in Secs. 4 and 5, respectively. In Sec. 6 a simple theoretical equation is obtained which relates the frequency and spin-lattice relaxation-time data. Spin-spin relaxation-time data are presented in Sec. 7.

2. APPARATUS AND EXPERIMENTAL TECHNIQUE

A pulsed magnetic resonance spectrometer is used to measure pure NQR frequencies and relaxation times. The 1-kW rf pulses delivered to the sample coil are provided by a conventional pulsed transmitter composed of a cw variable frequency oscillator, a gating circuit,[16] and a power amplifier. Appropriate combinations of Tektronix 160 series waveform generators are used to turn the transmitter on and off and thereby produce the desired pulse sequences. A Hewlett-Packard 5233L counter is used to measure the time interval between pulses.

The sequence of rf pulses is coupled to the sample coil through a rf bridge circuit[17] which matches the 50-Ω transmission line from the transmitter to the high Q sample coil and reduces the amplitude of the rf pulses at the input of the receiver to less than 1 V. The rf magnetic field set up within the sample space is able to saturate the chlorine resonances studied in ~10 μsec. The voltage subsequently induced back into the sample coil by the oscillating nuclear magnetization is coupled via the bridge to the receiver. The bridge matches the impedance of the sample coil to the 50-Ω input of the receiver.

The receiver consists of a low-noise (1.6 dB) preamplifier of bandwidth 2 MHz followed by a LEL IF20A main amplifier of bandwidth 10 MHz. Telonic TA-50A and TB-50A attenuators provide a gain control. Phase sensitive detection is obtained by mixing a reference signal with the nuclear signal. The reference signal, taken from the continuously running oscillator in the transmitter, is passed through a phase shifter[18] and attenuator and mixed with the nuclear signal in the first stage of the main amplifier. Following phase-sensitive detection, the nuclear signal is amplified by a video amplifier, monitored by an oscilloscope, and sampled and averaged by a boxcar integrator.[19] The output from the boxcar is recorded on a Hewlett-Packard 7101 BM strip-chart recorder.

To measure pure NQR frequencies the variable frequency oscillator is adjusted to resonance and its frequency measured by means of a Hewlett-Packard 3735A counter and a General Radio 1156A decade scalar. To obtain a coarse setting of the oscillator, the free-induction decay signal following a single rf pulse is viewed on the monitor oscilloscope and the oscillator frequency varied to eliminate the beats resulting from the interference of the nuclear signal with the reference signal. The final adjustment is made by observing the boxcar output and varying the oscillator frequency to maximize the free-induction decay amplitude. Using this technique resonance frequencies can be measured to within ±1 kHz.

For a powder sample the amplitude of a NQR free-induction decay signal following a single rf pulse of duration t_w varies with t_w. A first maximum, analogous to the response to a $\frac{1}{2}\pi$ pulse in NMR, occurs for $t_w(\frac{1}{2}\pi)=1.774/\sqrt{3}\gamma H_1$,[20] where γ is the nuclear gyromagnetic ratio and H_1 is the amplitude of the rf magnetic field. The next minimum, analogous to the

[9] C. E. Tarr, L. M. Stacey, and C. V. Briscoe, Phys. Rev. **155,** 272 (1967).
[10] F Bridges and W. G. Clark, Phys. Rev. **164,** 288 (1967).
[11] F. Bridges, Phys. Rev. **164,** 299 (1967).
[12] K. R. Jeffrey and R. L. Armstrong, Can. J. Phys. **44,** 2315 (1966).
[13] R. F. Tipsword and W. G. Moulton, J. Chem. Phys. **39,** 2730 (1963).
[14] T. E. Haas and E. P. Marram, J. Chem. Phys. **43,** 3985 (1965).
[15] D. Nakamura, Y. Kurita, K. Ito, and M. Kubo, J. Am. Chem. Soc. **82,** 5783 (1960).
[16] R. J. Blume, Rev. Sci. Instr. **32,** 554 (1961).
[17] K. R. Jeffrey and R. L. Armstrong, Rev. Sci. Instr. **38,** 634 (1967).
[18] W. G. Clark, Rev. Sci. Instr. **35,** 316 (1964).
[19] R. J. Blume, Rev. Sci. Instr. **32,** 1016 (1961).
[20] D. E. Woessner and H. S. Gutowsky, J. Chem. Phys. **39,** 440 (1963).

response to a π pulse in NMR, occurs for $t_w(\pi) = 3.629/\sqrt{3}\gamma H_1$.

The spin-lattice relaxation time T_1 is measured through the use of the sequence of two equal pulses of duration $t_w(\frac{1}{2}\pi)$ and variable separation τ suggested by Woessner and Gutowsky.[20] The amplitudes A_0 and A_1 of the free-induction decay signals as measured at a fixed time after the first and second pulses, respectively, are related to T_1 through

$$A_1 = A_0[1-\alpha \exp(-\tau/T_1)],$$

where α is a numerical coefficient. The continuous variation of A_1 with τ is traced out on the chart recorder as τ is swept from $\sim 0.1\ T_1$ to $\sim 2T_1$ at a rate which is slow compared to the effective time constant of the boxcar. To accomplish this, a modified Tektronix 162 waveform generator and the technique outlined by Blume[21] are used. Values of A_0 are determined both before and after each swept trace is taken. When T_1 becomes too long for this method to be practical (below 77°K in the present case) the boxcar is operated in a single shot mode. A "saturating comb" consisting of 10 5-μsec rf pulses is used to saturate the resonance and then a single pulse to monitor the recovery of the nuclear magnetization to its equilibrium value. The amplitude of the free-induction decay signal following the monitoring pulse is sampled just once by the boxcar for each value of τ. Using the methods outlined above T_1 values can be determined to within $\pm 3\%$ except at the very lowest temperatures where T_1 is the order of minutes. In the region below 50°K the probable error in T_1 is $\pm 7\%$.

The spin-spin relaxation time T_2 is measured by applying $t_w(\frac{1}{2}\pi) - t_w(\pi)$ pulse sequences with variable spacing τ and by tracing out the variation of the echo signal amplitude with τ. The echo amplitude at each value of τ is obtained by sweeping the sampling gate of the boxcar through the region of the echo. In the present experiments, the echo amplitudes were not observed to decay exponentially with τ. The analysis of the data to yield T_2 values will be discussed in Sec. 6.

The present experiments were carried out on two samples of K_2PtCl_6 obtained from Johnson, Matthey, and Mallory, Ltd. Although the free-induction decay-time constants T_2^* were different for the two samples, all of the other experimental quantities measured were independent of the sample. Furthermore, after a sample was maintained at a temperature $\sim$500°K for a few hours the value of T_2^* was found to have increased. Since T_2^* is governed by the inhomogeneity of the local electric field gradients at the sites of the resonant nuclei, the variation of T_2^* with sample and amount of heat treating probably results from differences in the strains within the constituent crystallites.

Measurements were carried out over the temperature range $6 < T < 490$°K. Below 6°K the T_1 values become too long and above 490°K too short to allow reliable measurements to be obtained in the manner described. Above 490°K the limitation is provided by the desaturation time of the receiver and below 6°K by the long-time stability of the spectrometer.

For temperatures $\sim$300°K the sample coil is placed inside a copper container around which a heater is wrapped. This container is placed inside a second one and the interspace evacuated. The two containers form a part of the bridge circuit and are joined to it by a thin-walled, stainless-steel tube $\frac{3}{4}$ in. in diameter which serves as the outer conductor of a transmission line coupling the bridge to the sample coil. A second thin-walled stainless-steel tube $\frac{1}{8}$ in. in diameter provides the center conductor. This sample assembly is placed within a Dewar which may utilize either liquid nitrogen or liquid helium as a coolant. A copper-constantan thermocouple is used to monitor the sample temperature. The thermocouple voltage is compared to a bucking voltage which is set for a particular temperature. The error voltage is monitored by a Hewlett-Packard 425 AR dc microvoltmeter, the output from which is amplified and supplied to the heater to maintain the desired temperature. With this temperature control system constant temperatures could be maintained to within $\sim\frac{1}{10}$°K.

For temperatures >300°K, a sample assembly having a relatively short length of transmission line is used and the Dewar is replaced by an oven.

3. ELECTRIC FIELD GRADIENT AT THE X SITES IN CUBIC R_2MX_6 COMPOUNDS

The cubic R_2MX_6 compounds have the antifluorite structure[22] as illustrated in Fig. 1(a). The Bravais lattice is fcc; the basis consists of one $[MX_6]^=$ ion at (0, 0, 0) and two R^+ ions at $\pm(\frac{1}{4}, \frac{1}{4}, \frac{1}{4})$. The $[MX_6]^=$ ion defines a regular octahedron as shown in Fig. 1(b). Since the environment of any X nucleus is one of axial symmetry, the electric field gradient at an X site is expected to possess axial symmetry.

For a particular Cl nucleus in K_2PtCl_6, the nearest neighbor is a Pt atom at a distance of 2.33 Å, the second nearest neighbors are four Cl nuclei at distances of 3.30 Å, and the third nearest neighbors are four K nuclei at distances of 3.44 Å.

Since in aqueous solution R_2MX_6 compounds form stable R^+ and $[MX_6]^=$ ions, it follows that the bonding within a $[MX_6]^=$ complex ion is much stronger than the bonding between R^+ and $[MX_6]^=$ ions. This observation has prompted previous workers[14,23,24] to express the X NQR frequencies in the form

$$\nu = \tfrac{1}{2}e^2 | Q(q_{ci} + q_{ni}) |,$$

[21] R. J. Blume, Rev. Sci. Instr. **32**, 743 (1961).

[22] W. G. Wychoff, *Crystal Structures* (Interscience Publishers, Inc., New York, 1965), 2nd ed., Vol. 3, p. 339.

[23] D. Nakamura and M. Kubo, J. Phys. Chem. **68**, 2986 (1964).

[24] R. Ikeda, D. Nakamura, and M. Kubo, J. Phys. Chem. **69**, 2101 (1965).

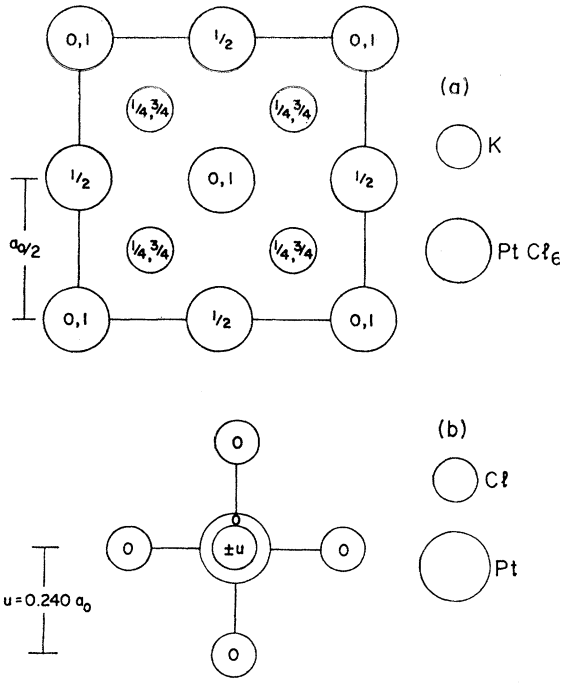

FIG. 1. (a) The structure of a cubic R_2MX_6 compound. The Bravais lattice is fcc; the basis consists of one $[MX_6]^=$ ion at (0, 0, 0) and two R^+ ions at $\pm(\frac{1}{4}, \frac{1}{4}, \frac{1}{4})$. A unit cube is shown projected on one face. (b) The octahedral arrangement of X atoms about the M atom in the $[MX_6]^=$ ion.

where e is the electronic charge, Q is the scalar nuclear quadrupole moment, and q_{ci}, q_{ni} are the parts of the electric field gradient at the X sites due to the complex ion and to the neighboring ions, respectively.

If we interpret q_{ci} to be due solely to the isolated complex ion, then according to the Townes and Dailey theory[25] we can write

$$q_{ci}=fq_{\text{atom}},$$

with

$$f=N_z-N_\pi.$$

In this expression q_{atom} is the electric field gradient at an X nucleus situated in an isolated X atom, which for halogen atoms results from the single unfilled p shell. N_z, the electron population in the p_z orbital about the X atom in the complex ion, is given by

$$N_z=1+s^2-d^2+I,$$

where s^2 is a measure of s hybridization (from the $3s^2$ state in Cl), d^2 is a measure of d hybridization (from the $3d_{zz}$ state in Cl), and I is the ionic character of the bond in the complex ion. N_π, the average electron population in the p_x and p_y orbitals, is given by

$$N_\pi=2-\pi,$$

where π is a measure of Π bonding in the complex ion. In K_2PtCl_6, $\pi=0$ so that f is a negative quantity. Since q_{atom} is -39.93×10^{24} cm^{-3},[26] q_{ci} is a positive quantity.

The quantity q_{ni} may be separated into direct and indirect parts. The direct part is calculated by taking the contribution to the field gradient at the site of the X nucleus due to point charges situated at the neighboring ion sites. It may be shown to be small.[23] A more important contribution to the field gradient may well result indirectly from the polarization of the electronic structure of the complex ion by the neighboring ions. Unfortunately, it is very difficult to make even an order-of-magnitude estimate of this indirect part and it is usually neglected.

4. PRESENTATION AND DISCUSSION OF THE FREQUENCY DATA

The NQR frequency was measured for both the ^{35}Cl and ^{37}Cl isotopes. The ratio of frequencies, $\nu(^{35}\text{Cl})/\nu(^{37}\text{Cl})$, has the constant value 1.2688 ± 0.0001 to within experimental error over the entire temperature range studied. This value is in agreement with the ratio of the quadrupole coupling constants found in atomic beam experiments on Cl atoms by Jaccarino and King,[27] 1.2686 ± 0.0004.

The experimental measurements for the ^{35}Cl isotope are presented in Fig. 2. The frequency is seen to decrease monotonically with increasing temperature. Bayer[2] has explained such a decrease for a simple case in which the atom containing the resonant nucleus executes a planar torsional oscillation about another atom to which it is

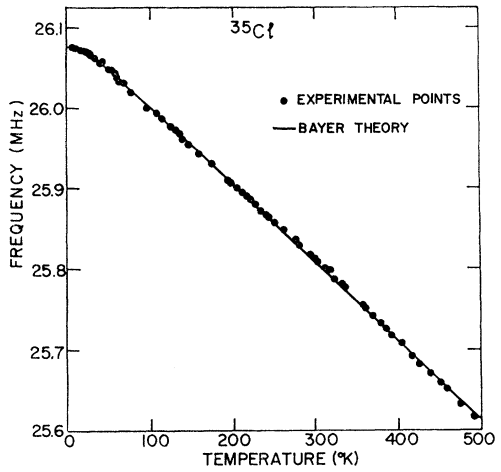

FIG. 2. A plot of the temperature variation of the NQR ^{35}Cl frequency in a powder sample of K_2PtCl_6. The solid curve is a simple Bayer theory fit for a torsional oscillation frequency of 38 cm^{-1}.

[25] T. P. Das and E. L. Hahn, in *Solid State Physics*, edited by F. Seitz and D. Turnbull (Academic Press Inc., New York, 1958), Suppl. 1, p. 131.

[26] T. P. Das and E. L. Hahn, in *Solid State Physics*, edited by F. Seitz and D. Turnbull (Academic Press Inc., New York, 1958), Suppl. 1, p. 127.

[27] V. Jaccarino and J. G. King, Phys. Rev. **83**, 471 (1951).

TABLE I. Summary of infrared and Raman data for K_2PtCl_6.

	Internal modes						Lattice modes		
Designation	ν_1	ν_2	ν_3	ν_4	ν_5	ν_6	T_1	T_2	R
Species	A_{1g}	E_g	F_{1u}	F_{1u}	F_{2g}	F_{2u}	F_{2g}	F_{1u}	F_{1g}
Activity	r	r	ir	ir	r	•••	r	ir	•••
Frequency (cm^{-1})	344	320	345	183	162	•••	•••	90	•••

bonded. The resonant nucleus is assumed to experience an axially symmetric electric field gradient which is a constant of the motion. The temperature dependence of the resonance frequency is described by the equation

$$\nu(T)=\nu_0[1-(3\hbar^2/4Ik\Theta_t)\coth(\Theta_t/2T)],$$

where ν_0 is the limiting static value of the resonance frequency, I is the moment of inertia of the torsional oscillator, Θ_t is the torsional oscillator frequency expressed as a temperature, and T is the absolute temperature. A least-squares fit of this equation to the experimental data yielded the parameters

$$\nu_0=26.102 \text{ MHz},$$

$$\Theta_t=55°\text{K (which corresponds to 38 cm}^{-1}),$$

$$I=1.1\times10^{-37}\text{ g cm}^2.$$

The Bayer equation for these parameters is shown by the solid curve in Fig. 2. Clearly this simple equation represents the data extremely well.

The above analysis suggests that a single low-frequency lattice mode dominates the motional averaging of the electric field gradient at a Cl site as observed in a NQR experiment. The unit cell of K_2PtCl_6 contains nine atoms, and therefore there are three acoustical and 24 optical-lattice modes to consider. Since the acoustical modes of K_2PtCl_6 can be characterized by a Debye temperature[28] in excess of 200°K, they will not be considered further. The inclusion of the acoustical modes in a more comprehensive analysis could result in small changes in the parameters deduced below. The optical modes can be subdivided into 15 internal modes and nine lattice modes. The available infrared and Raman data[29,30] on the optical vibrations are summarized in Table I. The internal modes are, in general, high-frequency modes. All of them except the inactive ν_6 mode have been observed and have frequencies in excess of 150 cm^{-1}. We are left to consider the lattice modes. The T_1 and T_2 modes are both translatory in nature and involve the motion of one sublattice against another. These two modes are expected to have similar frequencies. In K_2SnCl_6, for example, the T_1 and T_2 frequencies are 73 and 79 cm^{-1}, respectively.[30] The remaining rotary (R) mode corresponds to the threefold degenerate torsional oscillations of the $[PtCl_6]^=$ ion about its three axes of symmetry. A frequency of 38 cm^{-1} is certainly not unreasonable for such a mode. For instance, the frequencies of the planar torsional oscillations of the anions in inorganic nitrates and carbonates about their trigonal axes have been observed to occur in the range 15 to 30 cm^{-1}.[31] Furthermore, such a rotary motion would be expected to be relatively efficient for the motional averaging of the field gradient. Therefore we suggest that it is the rotary-lattice mode which dominates the observed temperature dependence of the NQR frequency.

Now that the F_{1g} mode of the $[PtCl_6]^=$ ion has been identified as being predominantly responsible for the temperature variation of the NQR frequency, a more realistic formula can be used to analyze the data. We assume that any contribution to the field gradient resulting from neighboring ions can be neglected.

Following Das and Hahn[32] we take space-fixed axes $x'y'z'$ and moving principal axes xyz for the field gradient tensor at a Cl site. The torsional oscillations of the $[PtCl_6]^=$ ion cause angular displacements θ_x, θ_y, θ_z of the xyz axes with respect to the $x'y'z'$ axes. If terms up to the fourth power of the angular displacements are retained, and if an average over the torsional motion is taken, then it may be shown that the field gradient parameter q' and the asymmetry parameter η' in the $x'y'z'$ coordinate frame are related to the corresponding parameters q and η in the xyz frame through[33]

$$q'=q[1-\tfrac{3}{2}(\langle\theta_x^2\rangle+\langle\theta_y^2\rangle)+\tfrac{1}{2}(\langle\theta_x^4\rangle+\langle\theta_y^4\rangle)+\tfrac{3}{2}\langle\theta_x^2\rangle\langle\theta_y^2\rangle],$$

$$\eta'=(q/q')[-\tfrac{3}{2}(\langle\theta_x^2\rangle-\langle\theta_y^2\rangle)+\tfrac{1}{2}(\langle\theta_x^4\rangle-\langle\theta_y^4\rangle)-\tfrac{3}{2}\langle\theta_x^2\rangle\langle\theta_y^2\rangle+\tfrac{3}{2}\langle\theta_z^2\rangle(\langle\theta_x^2\rangle-\langle\theta_y^2\rangle)].$$

[28] L. V. Coulter, K. S. Pitzer, and W. M. Latimer, J. Am. Chem. Soc. **62**, 2845 (1940).
[29] P. J. Hendra and P. J. D. Park, Spectrochim. Acta **23A**, 1635 (1967).
[30] M. Debeau and J. P. Mathieu, Compt. Rend. **260**, 5229 (1965).
[31] R. A. Schroder, C. E. Weir, and E. R. Lippincott, J. Res. Natl. Bur. Std. **66A**, 407 (1962).
[32] T. P. Das and E. L. Hahn, in *Solid State Physics*, edited by F. Seitz and D. Turnbull (Academic Press Inc., New York, 1958), Suppl. 1, p. 41.
[33] To second order, these expressions are identical to the expressions given in T. P. Das and E. L. Hahn, in *Solid State Physics*, edited by F. Seitz and D. Turnbull (Academic Press Inc., New York, 1958), Suppl. 1, p. 42.

For a threefold degenerate torsional oscillation these expressions reduce to

$$q' = q[1 - 3\langle\theta^2\rangle + \langle\theta^4\rangle + \tfrac{3}{2}\langle\theta^2\rangle^2],$$
$$\eta' = (q/q')[-\tfrac{3}{2}\langle\theta^2\rangle^2].$$

Since the NQR frequency depends upon η'^2, the effect of a nonzero η' is negligible to fourth order. For a quantum-mechanical torsional oscillator,

$$\langle\theta^2\rangle = E/I\omega_t^2,$$
$$\langle\theta^4\rangle = 3E^2/2I^2\omega_t^4 + 3\hbar^2/16I^2\omega_t^2,$$

and

$$E = \tfrac{1}{2}(\hbar\omega_t)\coth(\hbar\omega_t/2kT),$$

where E is the energy, ω_t the torsional oscillator frequency, and I the moment of inertia. Therefore the NQR frequency is given by

$$\nu = \nu_0\left\{1 - \frac{3\hbar^2}{2Ik\Theta_t}\coth\frac{\Theta_t}{2T} + \frac{3\hbar^4}{4I^2k^2\Theta_t^2}\left[\coth^2\frac{\Theta_t}{2T} + \frac{1}{4}\right]\right\},$$

with

$$\nu_0 = eQq/2h \quad \text{and} \quad \Theta_t = \hbar\omega_t/k.$$

Substitution of approximate values for the parameters reveals that for $T > 100°K$ the contribution to ν of the third term on the right-hand side > 1 kHz. Therefore this term should be retained in the analysis.

Thermal expansion of the lattice may also affect the temperature dependence of the NQR frequency since the experiments were carried out with the sample at constant pressure rather than at constant volume.[4] Since we are only considering the contribution to the field gradient coming from the complex ion and since an expansion of the lattice is most likely due to an increase of the distance between K^+ and $[PtCl_6]^=$ ions, therefore, to a first approximation, q and I are constants and only θ_t is temperature-dependent. That is, thermal expansion can be empirically taken into account by writing

$$\Theta_t = \Theta_t^0(1 - \alpha T),$$

where α is a coefficient of expansion.

The theoretical curve shown in Fig. 2, in terms of the model discussed, is given by

$$\nu = \nu_0[1 - (3\hbar^2/2Ik\Theta_t)\coth(\Theta_t/2T)].$$

This is just the simple Bayer theory formula with a redefined value of I to take account of the degeneracy of the F_{1g} mode. From this formula we obtain $I = 2.14\times10^{-37}$ g cm^2 as compared to a value $I_{calc} = 1.28\times10^{-37}$ g cm^2 as calculated from the geometry of the $[PtCl_6]^=$ structure.

A close examination of Fig. 2 reveals that the theoretical curve passes below the data in the temperature range $250 < T < 350°K$ and above the data for $T > 400°K$. The effect of including the third term in the theoretical expression for the NQR frequency is to raise the theoretical curve slightly at the higher temperatures. The effect of including the term to account for thermal expansion is to lower the theoretical curve at the higher temperatures. It is therefore reasonable to expect that the inclusion of these two correction terms might improve the agreement between theory and experiment. However, if account is taken of the accuracy of the data and of the number of adjustable parameters now available, it becomes clear that no meaningful results can come from a more detailed analysis. Furthermore, the discrepancy between the values of I as obtained from fitting the data and from geometrical considerations is too large to be accounted for by these correction terms. It is our belief that this discrepancy results from the failure of the model to include a contribution to the field gradient resulting from the presence of the neighboring ions.

5. PRESENTATION AND DISCUSSION OF THE T_1 DATA

T_1 was measured for both the ^{35}Cl and ^{37}Cl isotopes. The results are shown in Fig. 3. The measured T_1 values span seven orders of magnitude ranging from 100 μsec at 490°K to 20 min at 6°K. For convenience we define a low- and a high-temperature region. In the low-temperature region ($T < 320°K$),

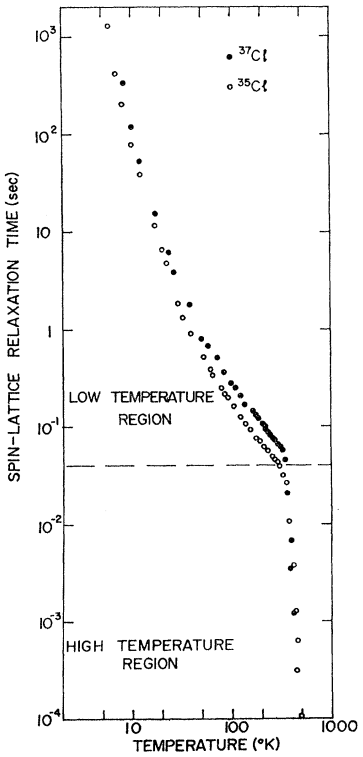

FIG. 3. A plot of the temperature variation of T_1 for the ^{35}Cl and ^{37}Cl isotopes in a powder sample of K_2PtCl_6. In the low-temperature region $T_1(^{35}Cl)/T_1(^{37}Cl) \simeq 1.6$; in the high-temperature region $T_1(^{35}Cl) \simeq T_1(^{37}Cl)$.

$T_1(^{37}Cl)/T_1(^{35}Cl)\simeq 1.6$. In the high-temperature region ($T>320°K$), $T_1(^{35}Cl)=T_1(^{37}Cl)$. The two regions are discussed separately.

Low-Temperature Region

The T_1 results for the low-temperature region are shown in more detail in Fig. 4. The insert shows the data for both isotopes in the temperature range $30<T<300°K$. The curve drawn through the ^{35}Cl points represents the best fit to the data. Based on this reference curve two other curves have been constructed which are labeled "magnetic" and "quadrupolar." The magnetic curve was obtained from the reference curve by dividing the value at each temperature by 1.44, the square of the ratio of the gyromagnetic ratios $\gamma(^{35}Cl)/\gamma(^{37}Cl)$. The quadrupolar curve was obtained in a similar manner, dividing by 1.61, the square of the ratio of the quadrupole moments $Q(^{35}Cl)/Q(^{37}Cl)$. It can be concluded that the dominant relaxation mechanism is quadrupolar in nature and results from the time-dependent portion of the electric field gradient at the Cl nuclear sites. The main set of points in Fig. 4 includes both the ^{35}Cl values and the ^{37}Cl values multiplied by 1.61.

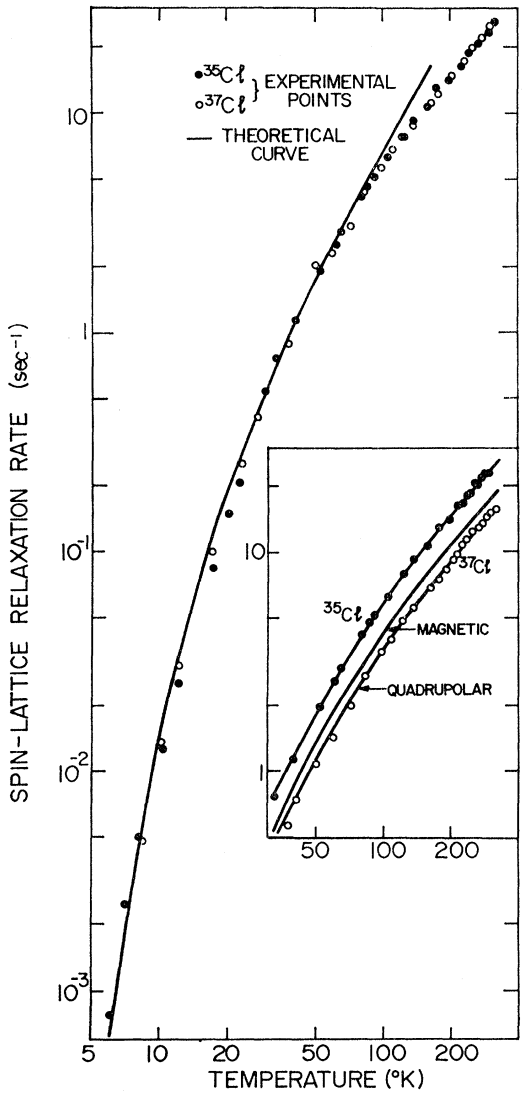

FIG. 4. The low-temperature T_1 region. The insert shows the predicted behavior of the ^{37}Cl T_1 data relative to the ^{35}Cl data assuming either a magnetic or a quadrupolar dominated relaxation mechanism. The latter assumption is clearly the correct one. In the main part of the graph the isotope dependence is suppressed. The solid curve assumes an Einstein phonon distribution at a frequency of 33 cm^{-1}.

Van Kranendonk[1] has derived a general theoretical expression for T_1 due to the interaction of a time-dependent crystalline electric field gradient with the nuclear quadrupole moments. In the theory, the lattice is assumed to consist of an array of point charges located at the lattice sites. All resonant nuclei are assumed to be at equivalent sites. The dependence of the field gradient at a resonant nucleus on the relative displacements of the nuclei from their equilibrium positions includes only the nearest neighbors. The lattice vibrations considered are restricted by the assumption that all nuclei are equivalent and hence that a unit cell can be chosen in such a fashion that it contains only one atom. The frequencies of the normal-lattice modes are assumed to be independent of the direction of the wave vector and the polarization. Effects such as covalency and antishielding are taken into account empirically by a multiplicative factor. Spin-lattice relaxation is assumed to result solely from Raman processes. The transition probability from a spin state m' to a state m, as given by a perturbation treatment, is

$$W_{mm'}=\frac{1}{\hbar^2}\iint\sum_{if}\{\,|\,\langle m,n_i+1,n_f-1\,|\,\mathcal{H}_{sl}\,|\,m',n_i,n_f\rangle\,|^2 \times\rho(\nu_i)\rho(\nu_f)\delta(\nu_i-\nu_f+\nu_0)\}d\nu_i d\nu_f.$$

In this expression $\mathcal{H}_{sl}$ is the Hamiltonian describing the spin-lattice coupling, n_i and n_f are the initial number of phonons at frequencies ν_i and ν_f, respectively, and $\rho(\nu_i)$ and $\rho(\nu_f)$ are the respective phonon density functions. The { } indicate an average over all directions of the wave vector and polarization. $W_{mm'}$ may be shown to be proportional to the phonon occupation numbers $\langle n_i\rangle_{av}$ and $\langle n_f+1\rangle_{av}$. Since phonons are bosons,

$$\langle n_i\rangle_{av}=[\exp(h\nu_i/kT)-1]^{-1}.$$

The nature of the spin-lattice coupling can be derived from a point-charge model and the assumptions concerning the nature of the lattice vibrations.

Following the procedure of Van Kranendonk, an estimate of the temperature dependence of T_1 in K_2PtCl_6 can be obtained. The contributions from the acoustical modes and the optical modes will be treated separately.

The acoustical modes involve the motion of the K^+

ions relative to the $[PtCl_6]^=$ ions. There are four K^+ ions nearest to each of the Cl nuclei within a $[PtCl_6]^=$ ion. The Cl nucleus lies only slightly above the plane of the four K^+ ions. Assuming that the Cl nucleus lies in this plane and representing the lattice vibration spectrum by a Debye model, it can be shown that the temperature dependence of T_1 is given by a weighted sum of the integrals

$$D_n = T^{*3} \int_0^{1/T^*} \frac{x^2 \exp x}{(\exp x - 1)^2} L_n(cT^*x)\, dx,$$

where $T^* = T/\Theta_D$, $c = (6\pi^2)^{1/3}$, Θ_D is the Debye temperature, and $n = 1, 2, 3, 4$. The functions $L_n(cT^*x)$ which result from an averaging of the spin-lattice coupling over the normal modes of vibration are given by Van Kranendonk.[1] The weighted sum of the D_n functions for the configuration considered here is proportional to the weighted sum found by Van Kranendonk[1] for the NaCl structure. Therefore,

$$T_1^{-1} \propto T^{*2} E^*(T^*), \tag{1}$$

with the function $E^*(T^*)$ as given by Van Kranendonk.[1]

The lattice vibration spectrum of each of the optical modes can be represented by an Einstein distribution. It is easily shown that for an Einstein distribution

$$T_1^{-1} \propto [\sinh(\Theta_E/2T)]^{-2}, \tag{2}$$

where Θ_E is the Einstein temperature. For K_2PtCl_6 the contribution to T_1 from the 24 optical modes involves a weighted sum of such expressions. The weighting must take account of the relative importance of each of the modes in the relaxation process. How this weighting should be carried out remains an unanswered question. If, however, a single optical mode dominates the relaxation process, the contribution to T_1 from the optical modes will reduce to expression (2).

Equations (1) and (2) were fitted to the data. For Eq. (1), the best fit corresponds to

$$T_1^{-1} = (3.5\ \text{sec}^{-1}\ ^\circ\text{K}^{-2})\, T^{*2} E^*(T^*),$$

with $\Theta_D = 64^\circ$K; for Eq. (2) the best fit corresponds to

$$T_1^{-1} = 0.40[\sinh(48/2T)]^{-2}\ \text{sec}^{-1}.$$

Each of the equations fits the data equally well. This is as expected since the two equations only begin to differ significantly for temperatures $<0.1\Theta_D$, where (1) predicts $T_1^{-1} \propto T^7$ and (2) predicts $T_1^{-1} \propto \exp(\Theta_E/T)$. Since a Debye temperature of 64°K is far too low for K_2PtCl_6,[28] it is reasonable to conclude that the relaxation process is dominated by a single optical mode characterized by $\Theta_E = 48^\circ$K, that is, a mode of frequency 33 cm^{-1}. The solid curve shown in the main part of Fig. 4 corresponds to the prediction of Eq. (2) for $\Theta_E = 48^\circ$K. Since a frequency of 33 cm^{-1} is in essential agreement with that of the mode responsible for the temperature variation of the NQR resonance frequency (38 cm^{-1}), it would seem as if the rotary-lattice mode dominates the temperature variation of both the NQR frequency and the low-temperature spin-lattice relaxation-time data.

Above 90°K, the T_1^{-1} data are not well represented by Eq. (2). The theoretical relaxation rate is increasing with temperature as T^2, whereas the experimental relaxation rate is increasing considerably more slowly than T^2. It should be noted that there is no way in which the general Van Kranendonk formulation can lead to a limiting high-temperature relaxation rate which increases with temperature more slowly than T^2. We suggest that above 90°K the amplitudes of oscillation of the chloroplatinate groups become large and the anharmonic nature of the oscillator potential well must be taken into account. The following analysis of the high-temperature region gives support for this conjecture.

High-Temperature Region

For $T > 320^\circ$K, T_1 becomes isotope-independent and decreases rapidly with increasing temperature. In Fig. 5, $\log T_1^{-1}$ is plotted as a function of T^{-1}. The "corrected" points are obtained from the measured ones by subtracting the small extrapolated contribution due to the torsional oscillation relaxation mechanism. The resulting plot is linear.

Alexander and Tzalmona[34] observed a similar temperature dependence of T_1 in hexamethylene tetramine. They attribute the behavior to a hindered rotation of the tetrahedral molecules. Let us assume that the torsional oscillations of the $[PtCl_6]^=$ ions, which seem to be responsible for the low-temperature region relaxa-

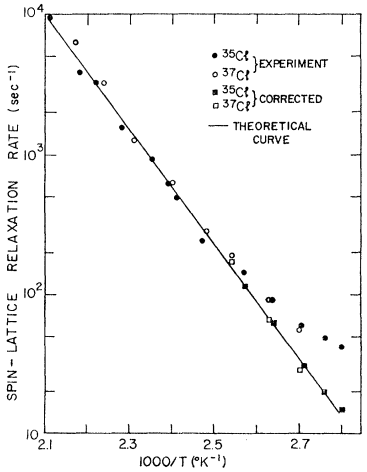

FIG. 5. The high-temperature T_1 region. The "corrected" points are obtained from the measured ones by subtracting a contribution due to the torsional oscillation relaxation mechanism. The theoretical curve corresponds to a barrier height to rotation of 9450°K and a moment of inertia of the hindered rotator of 5.64×10^{-37} g cm^2.

[34] S. Alexander and A. Tzalmona, Phys. Rev. **138**, A845 (1965).

tion, become hindered rotations for $T>320°K$ and that the hindered rotations are characterized by the conditions

$$\omega_Q \ll 1/\tau_t, \qquad \tau_r \gg \tau_t,$$

where ω_Q is the NQR frequency, τ_t is the time required to reorient the ion, and τ_r is the residence time, or time between reorientations, of the ion. The result of such rotations would be to transfer the Cl nuclei from one lattice site to another with an accompanying change in the direction of the electric field gradient but no change in its magnitude.

It has been pointed out by Matzkanin *et al.*[35] that the onset of such a hindered rotation does not cause any dramatic change in the variation of the NQR frequency with temperature. In particular, they did not find any marked change in the NQR frequency of hexamethylene tetramine due to the onset of the hindered rotation. However, such a hindered rotation provides a very efficient relaxation mechanism. We now derive approximate rate equations to describe the relaxation in K_2PtCl_6 following Alexander and Tzalmona.[34]

Assume that a Cl nucleus which starts out in a site ν' is rotated to a site ν while remaining in an eigenstate of the Hamiltonian appropriate to the nucleus at the initial site ν'. The eigenstates $|\beta\rangle_{\nu'}$ of the old Hamiltonian can be expressed as linear combinations of the eigenstates of the new Hamiltonian $|\alpha\rangle_\nu$ in the form

$$|\beta\rangle_{\nu'} = \sum_\alpha U_{\beta^{\nu'}\alpha^\nu} |\alpha\rangle_\nu,$$

where $|U_{\beta^{\nu'}\alpha^\nu}|^2$ is the probability of finding the nucleus in a state $|\alpha\rangle_\nu$ after the reorientation if it was initially in the state $|\beta\rangle_{\nu'}$. To obtain the rate equations, these probabilities are weighted by the appropriate Boltzmann factors for a thermal process. If the occupation number of the state $|\alpha\rangle_\nu$ is n_{α^ν}, then

$$dn_{\alpha^\nu}/dt = \sum_{\nu'} \sum_\beta (P_{\alpha^\nu\beta^{\nu'}} n_{\beta^{\nu'}} - P_{\beta^{\nu'}\alpha^\nu} n_{\alpha^\nu}),$$

where

$$P_{\alpha^\nu\beta^{\nu'}} = \omega_{\nu\nu'} |U_{\alpha^\nu\beta^{\nu'}}|^2 \exp[(E_\beta - E_\alpha)/2kT],$$

$$P_{\beta^{\nu'}\alpha^\nu} = \omega_{\nu'\nu} |U_{\beta^{\nu'}\alpha^\nu}|^2 \exp[(F_\alpha - E_\beta)/2kT],$$

with $\omega_{\nu\nu'}$ the probability that no change in the nuclear spin energy accompanies such a reorientation. If the equilibrium value $(n_{\alpha^\nu})_{eq}$ of n_{α^ν} is added and subtracted, if the exponentials are expanded to first order in $\hbar\omega_Q/kT$, and if it is noted that $|U_{\alpha^\nu\beta^{\nu'}}|^2 = |U_{\beta^{\nu'}\alpha^\nu}|^2$, then the rate equations take the form

$$d[n_{\alpha^\nu} - (n_{\alpha^\nu})_{eq}]/dt = \sum_{\nu'\beta} |U_{\alpha^\nu\beta^{\nu'}}|^2 (\omega_{\nu\nu'} n_{\beta^{\nu'}} - \omega_{\nu'\nu} n_{\beta^\nu})$$
$$- \sum_{\beta\nu'} \omega_{\nu'\nu} |U_{\alpha^\nu\beta^{\nu'}}|^2 [(n_{\alpha^\nu} - n_{\beta^\nu}) - ((n_{\alpha^\nu})_{eq} - (n_{\beta^\nu})_{eq})].$$

For Cl nuclei, $I=\frac{3}{2}$ and we define

$$P^\nu = n_{3/2^\nu} + n_{-3/2^\nu} - n_{1/2^\nu} - n_{-1/2^\nu}.$$

Since each Cl nucleus is in a site of cylindrical symmetry the Hamiltonian $\mathcal{H}_\nu$ is

$$\mathcal{H}_\nu = (e^2Qq/12) \times 3(I_{z_\nu}{}^2 - I^2).$$

When a Cl nucleus leaves a site ν the polarization leaves with it, but the Cl nucleus arriving at ν from ν' carries with it the polarization

$$P^\nu = [\tfrac{1}{2}(3\cos^2\theta_{\nu\nu'} - 1)] P^{\nu'},$$

where $\theta_{\nu\nu'}$ is the angle between z_ν and $z_{\nu'}$. The rate equations now take the form

$$d(P^\nu - P^\nu{}_{eq})/dt = \sum_{\nu'} \tfrac{1}{2}(3\cos^2\theta_{\nu\nu'} - 1)(\omega_{\nu\nu'} P^{\nu'} - \omega_{\nu'\nu} P^\nu)$$
$$- \tfrac{3}{2} \sum_{\nu'} \omega_{\nu'\nu} (1 - \cos^2\theta_{\nu\nu'}) (P^\nu - P_{eq}{}^\nu).$$

The sum over ν' is a sum over the contributions of the six Cl nuclei in the $[PtCl_6]^=$ ion. These may be labeled ±1, ±2, ±3, where $\pm i$ possess inversion symmetry with respect to the Pt nucleus. We assume that a one-step transition from $+i$ to $-i$ is not allowed but that all other transitions are equally probable. That is,

$$\omega_{\nu\nu'} = \omega_{\nu'\nu} = 1/\tau_r, \qquad \theta_{\nu\nu'} = \tfrac{1}{2}\pi, \qquad \nu' \neq -\nu$$
$$\omega_{\nu\nu'} = 0, \qquad \nu' = -\nu.$$

The rate equations then become

$$d(P^\nu - P_{eq}{}^\nu)/dt = - \sum_{\substack{\nu' \\ \nu' \neq -\nu}} (2\tau_r)^{-1} (P^{\nu'} - P^\nu)$$
$$- (6/\tau_r)(P^\nu - P_{eq}{}^\nu).$$

The first term on the right represents a cross-relaxation effect which tends to equalize the populations at the different sites ν. An rf pulse will not create the same polarizations at each of the six Cl sites since the axis of the sample coil does not make the same angle with all of the z_ν axes. However, the strong magnetic dipolar coupling between the nuclei (see Sec. 6) will very soon equalize the populations P^ν. That is, for $t > T_2$, $P^{\nu'} = P^\nu$ and

$$d(P^\nu - P_{eq}{}^\nu)/dt = - (6/\tau_r)(P^\nu - P_{eq}{}^\nu).$$

If this were not the case, the cross-relaxation terms would cause a nonexponential return of the polarizations P^ν to their equilibrium values. The experimental return to equilibrium was exponential to within experimental error.

The high temperature T_1 is therefore predicted to be

$$T_1 = \tfrac{1}{6}\tau_r.$$

To estimate τ_r we consider a hindered rotation about one of the symmetry axes of the $[PtCl_6]^=$ ion and assume that the four Cl atoms in the plane perpendicu-

[35] G. A. Matzkanin, T. N. O'Neal, and T. A. Scott, J. Chem. Phys. **44**, 4171 (1966).

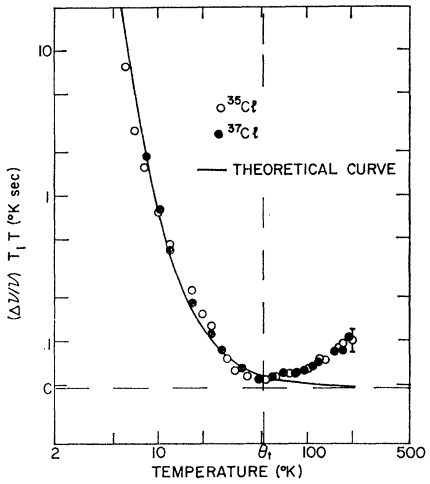

FIG. 6. A plot of $(\Delta\nu/\nu)T_1T$ versus T. The theoretical curve corresponds to $\Theta_t=51°K$ and $C=0.049°K$ sec.

lar to the axis of rotation establish a potential well of the form

$$V=\tfrac{1}{2}V_0(1+\cos 4\phi),$$

where V_0 is the height of the barrier to rotation. If the complex ion has sufficient energy to surmount the barrier, a hindered rotation will occur with angular frequency

$$\omega=(V_0/2I)^2,$$

where I is the moment of inertia. The time t required for the rotator to move from one potential well to another is

$$t=\tfrac{1}{4}(2\pi)(2I/V_0)^{1/2}.$$

An estimate of the jump time τ_r is given by the time t divided by the probability that the $[PtCl_6]^{=}$ ion will have the energy V_0. That is,

$$\tau_r=t\exp(V_0/kT)$$

and

$$\frac{1}{T_1}=\frac{12}{\pi}\left(\frac{V_0}{2I}\right)^{1/2}\exp\left(\frac{-V_0}{kT}\right).$$

This equation was fit to the data shown in Fig. 5 by the method of least squares. The resultant equation, with parameters

$$V_0=9.45\times10^3\ °K,$$

$$I=5.64\times10^{-37}\ g\ cm^2,$$

is shown by the solid line in Fig. 5. Considering the rough nature of the model used to estimate τ_r, the agreement between the fitted value of I and that calculated from the geometry of the $[PtCl_6]^{=}$ ion is reasonable.

6. SIMPLE THEORETICAL EQUATION FOR THE FREQUENCY AND SPIN-LATTICE RELAXATION-TIME DATA

The results of Secs. 4 and 5 indicate that the rotary optical mode dominates the temperature dependence of the resonance frequency and the spin-lattice relaxation time. Combining the Bayer theory equation for the temperature dependence of the NQR frequency and the Van Kranendonk equation for the temperature dependence of T_1, it follows that

$$(\Delta\nu/\nu)T_1T=C(\sinh 2\Theta^*/2\Theta^*),$$

where $\Delta\nu=|\nu-\nu_0|$, $\Theta^*=\Theta_t/T$, and C is a constant. It is interesting to note that the high-temperature limit of this expression is

$$(\Delta\nu/\nu)T_1T=C.$$

A best fit of an equation of this form to the low-temperature data, as shown in Fig. 6, yielded a value of $\Theta_t=51°K$ (35 cm^{-1}) and of $C=0.049°K$ sec. The failure of the Van Kranendonk theory for $T>90°K$ is clearly illustrated in this plot.

7. PRESENTATION AND DISCUSSION OF THE T_2 DATA

The decrease in the echo amplitude with τ is Gaussian for small τ. For long τ the decay is much slower than Gaussian and a slow beat pattern is observed. The spacing between the maxima in the beat pattern is in agreement with the value expected for "spin-echo beats"[36] in the magnetic field of the earth. The application of a larger magnetic field causes an increase in the number of beats and an increase in the length of the decay. It may therefore be concluded that T_2 is dominated by a magnetic dipolar spin-spin interaction. In a small magnetic field each of the nuclei will precess about the field which tends to average out the dipolar field as seen by a resonant nucleus and lengthen the decay.

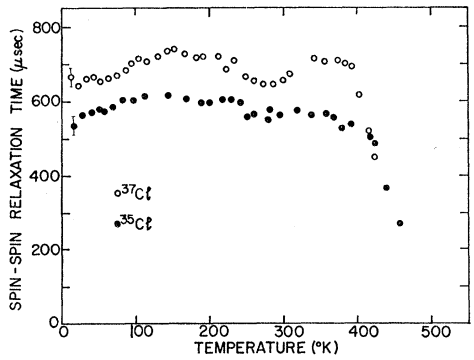

FIG. 7. A plot of the temperature variation of T_2 for the ^{35}Cl and ^{37}Cl isotopes in a powder sample of K_2PtCl_6. The ratio of the T_2 values for the two isotopes is ~1.20.

[36] T. P. Das and E. L. Hahn, in *Solid State Physics*, edited by F. Seitz and D. Turnbull (Academic Press Inc., New York, 1958), Suppl. 1, p. 77.

Values of T_2 were obtained from the data by fitting a Gaussian relation of the form

$$E=F_0\exp(-\tau/T_2)^2$$

to the first part of the decay when no external magnetic field was applied. A probable error of $\pm 5\%$ is associated with the values of T_2 deduced in this manner. The temperature dependence of T_2 is shown in Fig. 7. Over a large region of temperature T_2 is approximately constant with the values of 600 μsec for ^{35}Cl and 720 μsec for ^{37}Cl.

The experimental ratio of T_2 values for the two isotopes is 1.20. This agrees exactly with the isotopic ratio of gyromagnetic ratios which further substantiates that the behavior of T_2 is dominated by the dipolar interaction between neighboring nuclei.

8. CONCLUSIONS

We have seen that both the temperature dependence of the NQR frequency and spin-lattice relaxation data are dominated by the rotary optical mode of species F_{1g}. The analysis indicates that the frequency of this mode is approximately 35 cm^{-1}. Since this mode is neither infrared nor Raman active direct spectroscopic confirmation of this result would be difficult. If large enough single crystals were available a neutron scattering experiment could possibly confirm the analysis. Specific-heat measurements above 300°K should indicate the onset of a hindered rotation.

Other diamagnetic R_2MX_6 compounds could be expected to exhibit a similar behavior. The differences encountered would provide information leading to a more complete understanding of the lattice dynamics of these compounds. In particular, experiments on Cs_2PtCl_6 and Rb_2PtCl_6 should provide information on the importance of q_{ni} to the field gradient at a Cl site. Experiments carried out as a function of the applied hydrostatic pressure would clarify the importance of volume effects.

PHYSICAL REVIEW VOLUME 174, NUMBER 2 10 OCTOBER 1968

Spin-Lattice Relaxation in Pure and Europium-Doped BaF_2 Crystals at High and Low Temperatures*†

J. R. MILLER‡ AND P. P. MAHENDROO
Department of Physics, Texas Christian University, Fort Worth, Texas

(Received 5 April 1968)

The spin-lattice relaxation time T_1 of F^{19} has been measured in a pure BaF_2 crystal over a temperature range of 300 to 1150°K and in a BaF_2 crystal containing 4.9×10^{19} ions/cm^3 of Eu^{3+} from 4.2 to 1000°K. The measurements were made at 29 MHz using the magnetic-recovery method with the magnetic field along the [111] and [100] crystallographic directions. The electronic relaxation time τ_e of the europium was also measured at 9.5 gHz at 4.2, 63, 77, and 90°K. The data indicate that the diffusion of F^- ions provides the predominant relaxation mechanism above 700°K in the pure sample and above 500°K in the doped one. The minimum in the high-temperature segment of the T_1-versus-T curve appears at 990°K for pure BaF_2 and at 800°K for doped BaF_2. These yield jump frequencies of ν_F(vacancy) $=1.3\times10^{15}\exp(-1.35$ eV/kT) and ν_F(interstitial) $=6.5\times10^{11}\exp(-0.62$ eV/kT); to our knowledge these have never been measured before. Below 500°K the nuclear relaxation is due to paramagnetic impurities. The orientation dependence of T_1 indicates that the transition from "diffusion limited" (DL) to "rapid diffusion" (RD) relaxation occurs between 50 and 70°K in the doped sample. In the DL range, we find good agreement between the observed T_1 of F^{19} and the T_1 values calculated from τ_e, whereas at 4.2°K, which lies in the RD range, the calculated value is 300 times larger than the observed one. Our low-temperature T_1 data yield 5.6×10^{-14} cm/sec for the spin-diffusion constant D.

I. INTRODUCTION

SPIN-LATTICE relaxation mechanisms in solids can be determined by the dependence of the spin-lattice relaxation time T_1 on temperature. At high temperatures, the relaxation of dipolar nuclei in ionic solids, such as BaF_2, is due to fluctuations in the dipole-dipole coupling caused by the random jumping of the like and unlike magnetic nuclei. Torrey[1] has considered these interactions between only like nuclei and averaged over the angle θ between the radius vector connecting nuclei and the direction of the external magnetic field H. Eisenstadt and Redfield[2] have extended the theory to include interactions between like as well

* Research supported by the Air Force Office of Scientific Research, Office of Aerospace Research, United States Air Force, under AFOSR Grant No. 604-66.

† Based on a dissertation submitted in partial fulfillment of the requirements for the degree of Doctor of Philosophy by J. R. Miller to the Graduate Faculty of Texas Christian University. Reported in part in Bull. Am. Phys. Soc. **11**, 835 (1966). Some of the preliminary data were published in Phys. Letters **23**, 535 (1966).

‡ NDEA Fellow, 1962–65. Now at East Tennessee State University, Johnson City, Tenn.

[1] H. C. Torrey, Phys. Rev. **93**, 962 (1953).
[2] M. Eisenstadt and A. G. Redfield, Phys. Rev. **132**, 635 (1963).